Structural Engineering and Mechanics, Vol. 5, No. 4 (1997) 399-414
DOI: http://dx.doi.org/10.12989/sem.1997.5.4.399

Seismic performance of a fiber-reinforced plastic cable-stayed bridge

Osama A. Hodhod†

Department of Structural Engineering, Cairo University, Giza, Egypt

Magdi A. Khalifa†

Department of Civil Engineering, University of the United Arab Emirates, El-Ain, U.A.E.

Abstract. This paper presents an investigation into the seismic response characteristics of a proposed ligh-weight pedestrian cable-stayed bridge made entirely from Glass Fiber Reinforced Plastics (GFRP). The study employs three dimensional finite element models to study and compare the dynamic characteristics and the seismic response of the GFRP bridge to a conventional Steel-Concrete (SC) cable-stayed bridge alternative. The two bridges were subjected to three synthetic earthquakes that differ in the frequency content characteristics. The performance of the GFRP bridge was compared to that of the SC bridge by normalizing the live load and the seismic internal forces with respect to the dead load internal forces. The normalized seismically induced internal forces were compared to the normalized live load internal forces for each design alternative. The study shows that the design alternatives have different dynamic characteristics. The light GFRP alternative has more flexible deck motion in the lateral direction than the heavier SC alternative. While the SC alternative has more vertical deck modes than the GFRP alternative, it has less lateral deck modes than the GFRP alternative in the studied frequency range. The GFRP towers are more flexible in the lateral direction than the SC towers. The GFRP bridge tower attracted less normalized base shear force than the SC bridge towers. However, earthquakes, with peak acceleration of only 0.1 g, and with a variety of frequency content could induce high enough seismic internal forces at the tower bases of the GFRP cable-stayed bridge to govern the structural design of such bridge. Careful seismic analysis, design, and detailing of the tower connections are required to achieve satisfactory seismic performance of GFRP long span bridges.

Key words: bridges; long span bridges; cable-stayed; cable-structures; advanced composite materials; FRP; analysis; seismic; response.

1. Introduction

Glass Fiber Reinforced Plastics (GFRPs) are gaining grounds as reliable construction materials for the bridges of today and the future. Seible, *et al.* (1994) and Khalifa, *et al.* (1993) reported that short span bridges have been designed and constructed in recent years in China, Europe and the United States to demonstrate the potential of GFRPs as competent construction materials. The Aberfeldy Links Leader pedestrian cable-stayed bridge of Scotland is the first long span bridge in the world to be built entirely using GFRP (Seible, *et al.* 1994, and Head 1992). Khalifa

† Assistant Professor

and Tadros (1994) pointed out that, a few long span GFRP bridges have been under investigation in the United States such as the Lincoln Composite Bridge and the University of California-San Diego Bridge.

The above mentioned bridge projects have been made possible because of the collective intensive research work conducted in the last two decades on the mechanical and structural behavior of Advanced Composite Material (ACM). Previous research works of Mossallam (1993), Heger and Chambers (1984), and Mossallam and Chambers, (1994) have focussed extensively on the different aspects of the behavior of ACM under static loads. To the knowledge of the authors, very few published papers have dealt with the dynamic behavior of ACM systems for infrastructure applications such as the work of Mossallam and Abdel-Hamid (1993).

Cable-stayed bridges have acquired popularity around the world as a viable bridge design for medium to long span crossings. Their aesthetic form, competitive cost, and the efficient and fast mode of construction are some of the reasons behind their increasing popularity. However, traditional long span bridges (suspension and cable-stayed) made of steel or concrete are inherently flexible and more susceptible to dynamic loads induced by earthquakes, wind, and traffic than short span bridges (Scanlan 1987). The dynamic and seismic response characteristics of cable-stayed bridges have been studied by many researchers. Abdel-Ghaffar and Nazmy (1987) studied the effects of three dimensionality and non-linearities of cable-stayed bridges on their seismic response. Nazmy and Abdel-Ghaffar (1990a) formulated the equations of motion for two 3-D hypothetical models of cable-stayed bridges taking into account several sources of non-linearities. Abdel-Ghaffar and Nazmy (1990b) studied the seismic behaviour of the two models under synchronous and non-synchronous ground motions. Wilson and Gravelle (1991) modeled the Quincy Bayview Bridge, Quincy, Illinois, using linear 3-D finite elements to simulate its dynamic characteristics and found good agreement between their model and the results of an ambient vibration study conducted on the same bridge (Wilson and Liu 1991).

When considering GFRP as a construction material for a long span bridge, it should be noted that GFRPs have low elastic moduli and light weight compared to steel or concrete. The long term Young's modulus of GFRP is 1/4 that of concrete and 1/20 that of high strength steel. The weight of GFRP is 2/3 of concrete and 1/5 of steel. The stiffness and inertial properties of a GFRP long span bridge are expected to differ significantly from those of a traditional long span bridge (SC) made of reinforced concrete deck supported by steel main girders and has steel cables attached to reinforced concrete towers. This study compares the dynamic characteristics and the seismic response of two design alternatives, GFRP and SC, of a recently proposed cable-stayed pedestrian bridge (the Lincoln Composite Bridge). The comparison is conducted to evaluate the seismic performance of the two bridge design alternatives and judge the advantages of using GFRP in design situations where seismic forces are anticipated. The proposed bridge will be constructed with a total length of 274 m (900 ft) to connect two parts of a commuter trail near the south end of the city of Lincoln, Nebraska. The bridge will cross a state highway, major street, a park, and rail road tracks. The bridge will enhance the safety of pedestrians and commuters at this intersection (Khalifa and Tadros 1994).

2. The two bridge design alternatives

Two design alternatives of the same pedestrian cable-stayed bridge were developed namely,

Glass Fiber Reinforced Plastic (GFRP) and Steel-Concrete (SC). the bridge has a main span of 122 m (400 ft) and two side spans of 76 m (250 ft). The bridge's general lay-out is shown in Fig. 1.

The GFRP bridge has a honey-comb plate deck supported by honey-comb cross beams. The cross beams are attached to Aramid fiber stay cables. The towers are filament wound glass fiber reinforced plastic tubes. Fig. 2 shows the dimensions of the different sections of this design alternative. More details are reported by Khalifa and Tadros (1994). The SC bridge has a reinforced concrete deck supported by steel cross beams. The cross beams are carried by steel main girders. Steel stay cables are used to support the deck. The towers are designed to be reinforced concrete. Fig. 3 shows the dimensions of different sections of the SC bridge.

The two alternatives are dimensioned so that they have the same maximum deck deflection under live loads. This is the governing design criterion used by practitioners for the design of long span cable-stayed bridges due to their relatively high flexibility.

The two design alternatives are modeled using three dimensional (3-D) finite elements to study their vibrational characteristics and their behavior under different seismic excitations. In each model, the deck is represented by two spines that are properly spaced to preserve the inertial and stiffness properties of the deck sections. The towers are also modeled using 3-D beam elements while the cables are represented by using 3-D truss elements. The deck is assumed to be floating in the longitudinal direction at the towers and hinged at the end abutments.

This study assumes linear dynamic bridge behaviour. The effect of this assumption has been discussed by Nazmy and Abdel-Ghaffar (1987). Geometric non-linear behavior may result from cable sag effect, large amplitude displacements and P-Δ effects in the towers. Nazmy and Abdel-Ghaffar (1987) reported that linear dynamic analysis is sufficiently accurate for cable-stayed bridges with main spans up to approximately 500 m. This main span length includes almost all existing cable-stayed bridges. Abdel-Ghaffar and Khalifa (1991) studied the effect of cable vibration on the dynamic characteristics of cable-stayed bridges. It can be understood from their work that, cable vibrations, although having an importance in their own right, do not seem to significantly affect the global dynamic behaviour of the deck or towers. A single finite element representation of each cable appears to be sufficient for dynamic modeling of the deck or towers.

To meet the maximum deflection criterion, it was required to provide vertical support at the locations of the outer three back stays. These vertical supports are modeled as one dimensional

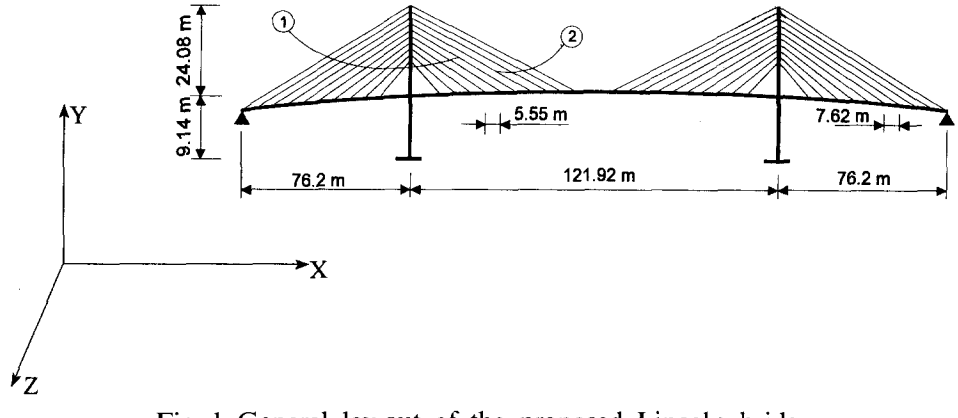

Fig. 1 General lay-out of the proposed Lincoln bridge.

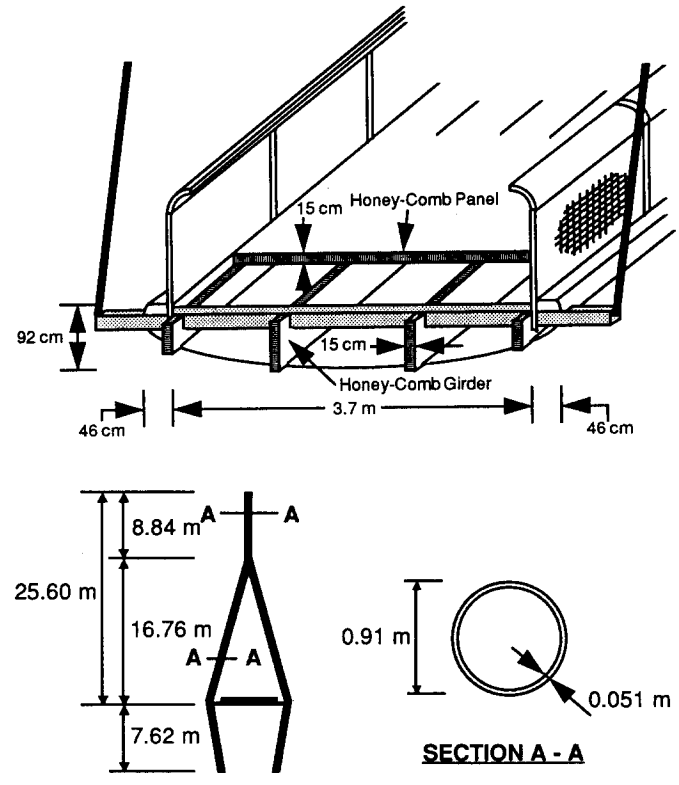

Fig. 2 Dimensions of the GFRP design alternative.

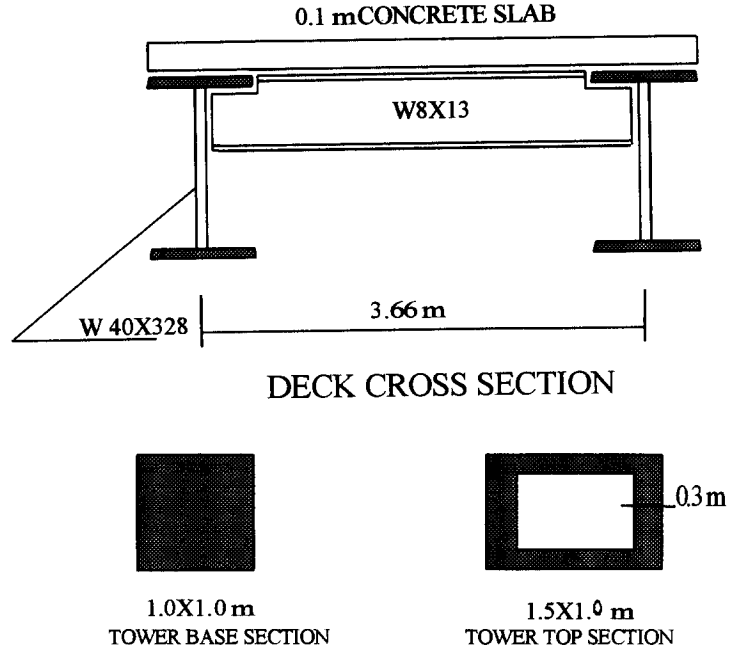

Fig. 3 Dimensions of the SC design alternative.

struts.

The finite element models' sectional properties (inertial and stiffness) are summarized in Table 1 for the two alternatives under investigation.

3. Dynamic characteristics of the two design alternatives

The linear eigenvalue problem was solved for the two models. The lowest 60 mode shapes of the two alternatives and their frequencies were extracted. The two design alternatives have different sequence of modes, some distinguished modes and different frequency ranges. The GFRP alternative has a very low frequency first lateral symmetric deck mode with frequency of 0.3719 Hz. This mode is followed by asymmetric vertical deck mode with a frequency of 0.8736 Hz. The SC alternative has a first vertical symmetric deck mode with a frequency of 0.7857 Hz followed by a lateral symmetric mode with a frequency of 0.9362 Hz. It appears, from the frequency values of the deck modes, that it can not be generally concluded, from a dynamics view point, that the GFRP deck is more flexible than the SC deck. The low GFRP tower mass and stiffness have caused higher GFRP first symmetrical vertical deck frequency compared to the SC deck vertical frequency. The tower contribution to the deck lateral stiffiness is minimum and the lateral bending stiffness of the GFRP deck is small compared to the lateral stiffness of the SC deck, as shown in Table 1, and this is the reason for the very low frequency first lateral GFRP mode. Fig. 4 shows some of the distinguished mode shapes of the two design alternatives. Fig. 5 compares the frequencies of the mode shapes of the two bridge design alternatives. Frequencies, modal masses and classification of selected modes are given in Table 2. Some tower modes in the longitudinal and lateral directions for both design alternatives are detected in the mode sequence. The GFRP first lateral tower mode, appears as the eighth mode in the mode sequence, has a frequency of 1.6265 Hz and the first longitudinal tower mode, appears as the eighteenth mode in the mode sequence, has a frequency of 2.8124 Hz. The SC first lateral tower mode, appears as the eighth mode in the mode sequence, has a frequency of 2.1496 Hz and the first logitudinal tower mode, appears as the ninth mode in the mode sequence, has a frequency of 2.3746 Hz. The GFRP first longitudinal tower mode has approximately double the amount of effective mass that is excited by the SC first longitudinal tower mode. The great difference in the effective modal mass reflects a big change in the mode shapes of the tower modes of the two design alternatives which is a result of the different mass and stiffness distribution within the two design alternatives.

The differences between the dynamic characteristics of the two models are expected to affect their seismic responses. a preliminary assessment of the differences in seismic response can be deduced from the distribution of the effective modal mass of the different mode shapes. The effective modal mass for mode j and global direction m is defined as (Habibullah and Wilson 1989)

$$\%EM_{jm} = \frac{\left(\sum_i M_{im}\,\phi_{imj}\right)^2}{\sum_i M_{im}\,\phi_{imj}^{\,2}} * \frac{100}{\sum_i M_{im}} \tag{1}$$

where,

Table 1 Cross section properties of the two 3-D finite element models

Element	FRP Alternative						SC Alternative					
	$A(m^2)$	$I_y(m^4)$	$I_z(m^4)$	$J(m^4)$	E(GPa)	G(GPa)	$A(m^2)$	$I_y(m^4)$	$I_z(m^4)$	$J(m^4)$	E(GPa)	G(GPa)
Cable 1	0.0001	–	–	–	110.21	–	0.0001	–	–	–	206.84	–
Cable 2	0.0013	–	–	–	110.21	–	0.0012	–	–	–	206.84	–
Deck spine	0.0658	0.0079	0.0666	0.0231	8.61	1.46	0.0621	0.0111	0.1163	0.0008	206.84	79.55
Tower base	0.1458	0.0150	0.0150	0.0132	8.61	1.46	0.8360	0.0833	0.0833	0.0983	30.79	12.31
Tower top	0.175	0.0474	0.0474	0.0327	8.61	1.46	1.1400	0.1202	0.2570	0.3106	30.79	12.31

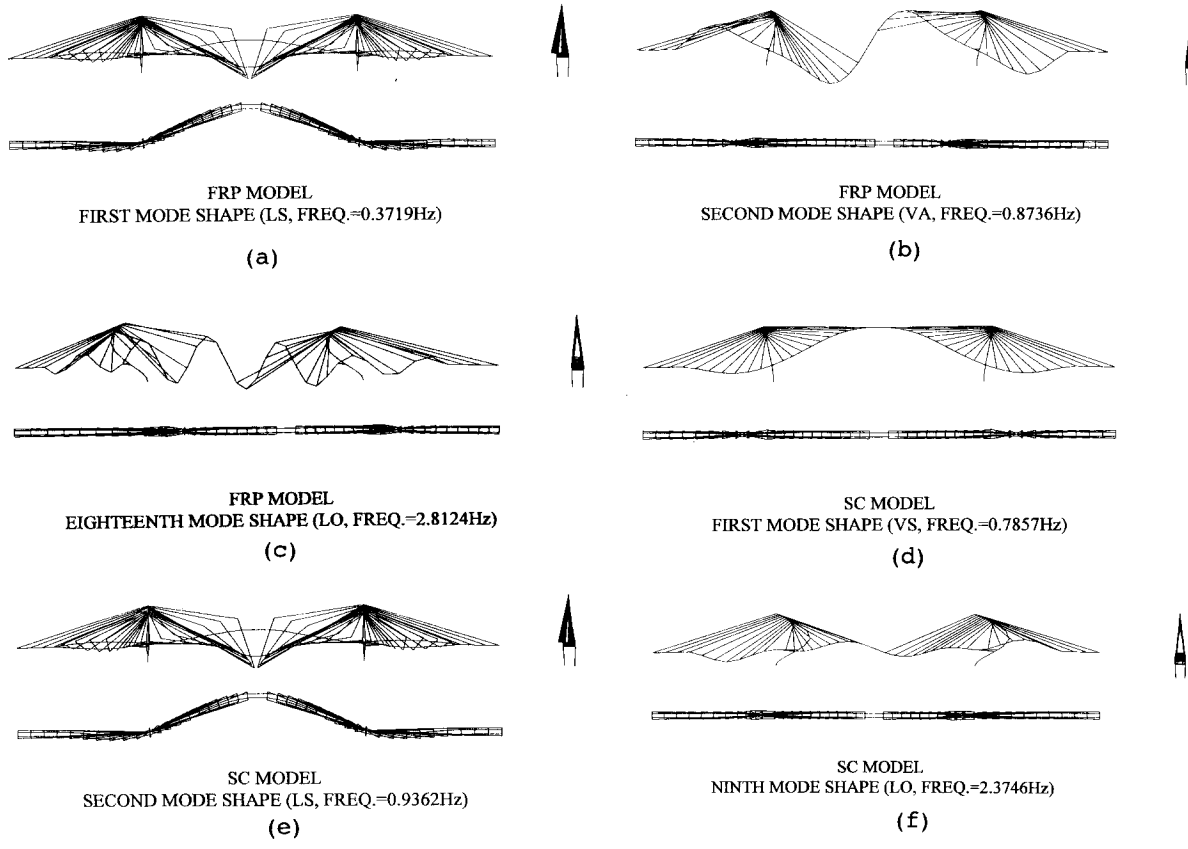

Fig. 4 Selected mode shapes of the two design alternative.

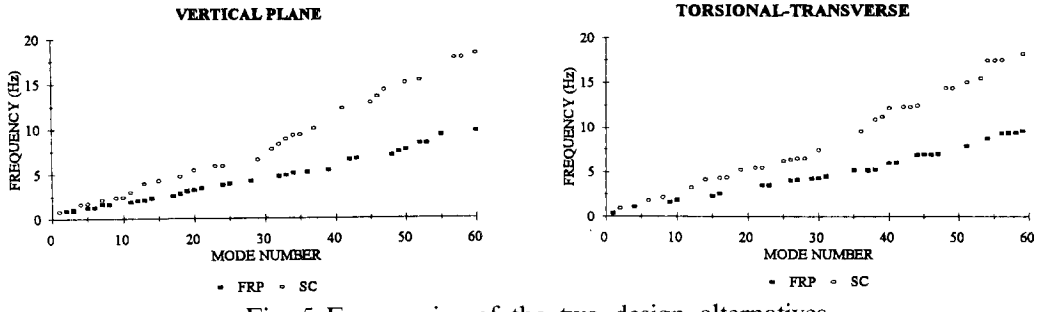

Fig. 5 Frequencies of the two design alternatives.

Table 2 Most contributing modes for the two design alternatives

GFRP Alternative						SC Alternative					
Mode	Freq. (Hz)	%EM$_x$*	%EM$_y$*	%EM$_z$*	Classification	Mode	Freq. (Hz)	%EM$_x$*	%EM$_y$*	%EM$_z$*	Classification
1	0.3719	–	–	27.197	LS	1	0.7857	.–	15.216	–	VS
6	1.2495	–	45.170	–	VS	2	0.9362	–	–	38.8	LS
8	1.6265	–	–	46.875	LS-LT	4	1.6237	–	16.325	–	VS
14	2.2922	–	6.515	–	VS	7	2.1114	–	12.377	–	VS
16	2.5589	–	–	2.927	LT	8	2.1496	–	–	34.387	LT
17	2.5730	12.386	–	–	LO	9	2.3746	26.431	–	–	LO
18	2.8124	68.069	–	–	LO	20	5.4209	16.371	–	–	LO
21	3.4362	–	6.722	–	VS	24	5.8625	5.789	–	–	LO
50	7.6606	5.131	–	–	LO	29	6.5654	34.423	–	–	LO
59	9.6215	–	–	1.165	LT	33	8.8654	–	4.599	–	VS
Total$^+$	–	90.666	69.600	83.380	–	Total$^+$	–	92.500	53.040	84.006	–

* Percentage of effective modal mass in the specified global direction
$^+$ total cumulative effective modal mass for the 60 modes
VS vertical symmetric deck mode
LS lateral symmetric deck mode
LO longitudinal tower mode
LT lateral tower mode

m X, Y, or Z global directions.
I structural node number.
j mode number
M_{im} translational mass associated with the i^{th} node in the global m direction.
ϕ_{imj} translational component at the i^{th} node in the global m direction of the j^{th} mode shape.

The effective modal mass ($\%Em_{jm}$) measures the percentage of the total mass that is excited by the j^{th} mode shape in the m^{th} global direction. This interpretation implies that its value represents the percentage of the total response that is expected to come from the j^{th} mode shape in the m^{th} global direction.

The distribution of the effective modal mass of the different mode shapes of the two design alternatives over the frequency range from 0-10 Hz is presented graphically in Fig. 6. Examining Fig. 6 shows that very few modes contribute to the response in each direction. The contributing modes are corresponding to the jumps in the effective modal mass values. However, collectively, many modes (especially for the SC alternative) are required to assure that the response is described reasonably.

The 60 modes considered in this study contain the following percentages of the effective modal mass for the GFRP alternative:

90.66 percent of the total effective mass in the longitudinal direction (M_x),
69.60 percent of the total effective mass in the vertical direction (M_y), and
83.38 percent of the total effective mass in the transverse direction (M_z).

The same number of modes contains the following percentages of the total effective modal mass for the SC alternative:

92.50 percent of the total effective mass in the longitudinal direction (M_x),

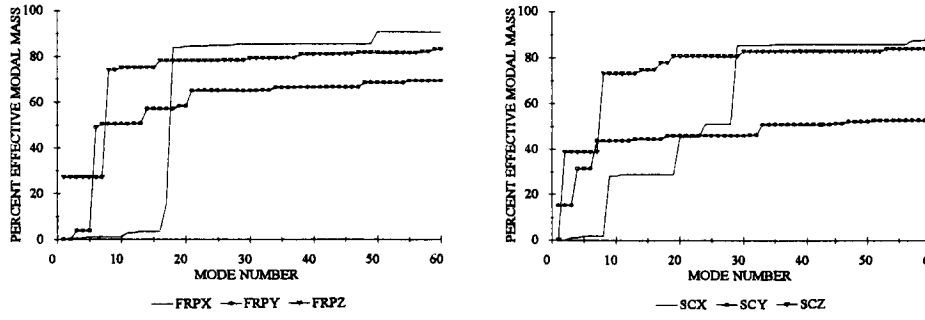

Fig. 6 Effective modal mass of the two design alternatives.

53.04 percent of the total effective mass in the vertical direction (M_y), and
84.00 percent of the total effective mass in the transverse direction (M_z).

These amounts of the effective modal mass are enough for the seismic response study purposes for two reasons: the first reason is that the included modes cover the frequency range from 0-10 Hz which is the effective frequency range for most earthquakes; and the second reason is that they include more than two tower modes in each of the longitudinal and lateral directions. Hodhod (1993) showed that the inclusion of the tower modes is inevitable to conduct reliable seismic analysis. A summary of the most contributing modes of the two models, their frequencies and mode calssification is shown in Table 2. It appears that for the GFRP alternative, effective modes have frequencies less than 3.0000 Hz. However, for the SC alternative, the effective modes are spread over the frequency range from 0.7857 Hz to 6.5654 Hz. It also shows that the vertical response of the GFRP alternative will depend primarily on the sixth mode which has 45 percent of the total M_y and that the longitudinal response of the GFRP alternative will depend primarily on the seventeenth and eighteenth modes that have more than 80 percent of M_x. This is not the case for the SC alternative because it does not have mode shapes with such high percentage of the effective modal mass. These results show that the frequency content of the ground motion will have an influence on the seismic response of the two design alternatives.

4. Ground motions

Earthquake ground motion records may be characterized by parameters such as peak ground acceleration in g (A), peak ground velocity in m/sec (V), frequency content, strong motion duration, spectrum intensity, earthquake magnitude, and earthquake epicentral distance. a simple characterization used in previous studies and used in the National Building Code of Canada is the A/V ratio (Tso, *et al.* 1992, Naumoski, *et al.* 1988). According to Naumoski, *et al.* (1988), High A/V ground acceleration records are associated with small or moderate earthquakes at short epicentral distances and Low A/V ground acceleration records are associated with moderate or large earthquakes occuring at large epicentral distances.

To prepare the ensemble of input ground accelerations, thirty three actual ground acceleration records divided into three frequency content categories, Low A/V, High A/V, and, Intermediate A/V, were available from the McMaster University Seismic Executive Data base (MUSE). The ground acceleration records were analyzed and the mean response spectra of each category

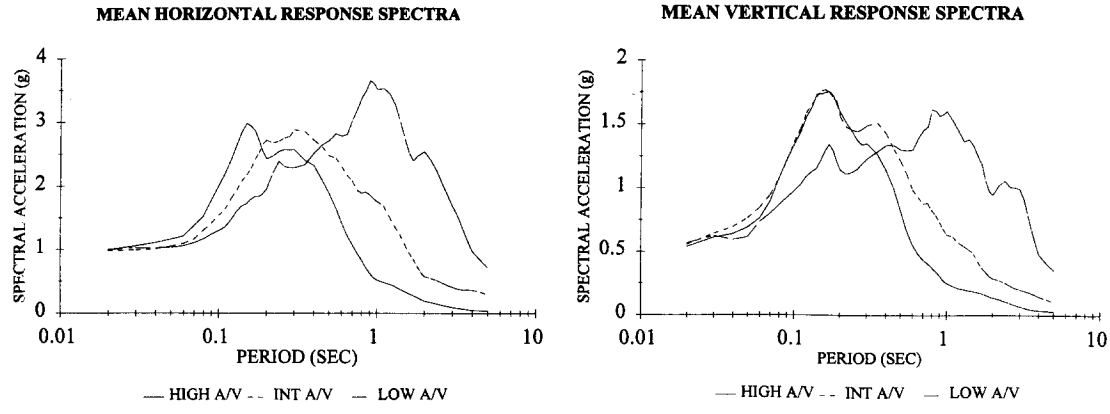

Fig. 7 Acceleration response spectra.

were calculated and scaled to a common peak ground acceleration of 0.1 g and used to generate an ensemble of three synthetic ground acceleration records, one for each category of frequency content (Hodhod 1993). It was decided to use synthetic ground acceleration records to represent the statistical average acceleration spectral properties of each *A/V* category. To generate a synthetic ground acceleration record, a target acceleration spectrum and a seed time history record were required. The target spectra used in the generation process were the mean acceleration response spectra of the data set in the MUSE database calculated for 5 percent damping as shown in Fig. 7. Characteristics of the seed time history records are presented in Table 3. Fig. 8 shows the ground acceleration components of the three synthetic records. The synthetic records were scaled to maximum accelerations $A1=0.1$ g (first horizontal component), $A2=0.09$ g (second horizontal component), $A3=0.06$ g (vertical component) in order to match the statistical relation between the three ground acceleration components of real earthquakes and also to simulate the seismicity of the bridge location. This scalling is referred to as the 0.1 g input.

5. Seismic time history analysis

Each synthetic ground acceleration record was applied to each of the two bridge models under study. The horizontal ground acceleration component with peak acceleration of 0.1 g was applied in the direction of the longitudinal bridge axis. The second horizontal ground acceleration component was applied in the transverse direction of the bridge and the vertical component in the vertical direction. Uniform base excitation was assumed in all cases. It was suitable to assume uniform ground excitation because of the relatively short length of the bridge's main span.

Modal time history analysis was used to estimate the seismic reponse of the two bridge models. Modal damping was assumed at 5 percent of critical for both models. This value was chosen bacause it reflects the amount of damping usually assumed in the design. It is noteworthy that research work is required to verify this value for both design alternatives. All generated 60 modes were used in the seismic response calculation. The amount of cumulative effective modal mass that is excited by these modes has appeared enough for the seismic response calculations as discussed earlier.

Table 3 Ground acceleration characteristics of the seed time histories

Record No.	Earthquake	Date	Site	Frequency content category	1st Horizotal A/V	Epic.	Soil distance (km)	Cond.
1	San Fernando	Feb., 9, 1971	800 W., 1st., L.A., Cal.	Low	0.50	6.4	41	Rock
2	Parkfield, California	June, 27, 1966	Temblor	High	1.86	5.6	7	Rock
3	Imperial Valley, California	May, 18, 1940	El Centro	Int.	1.04	6.6	8	Stiff Soil

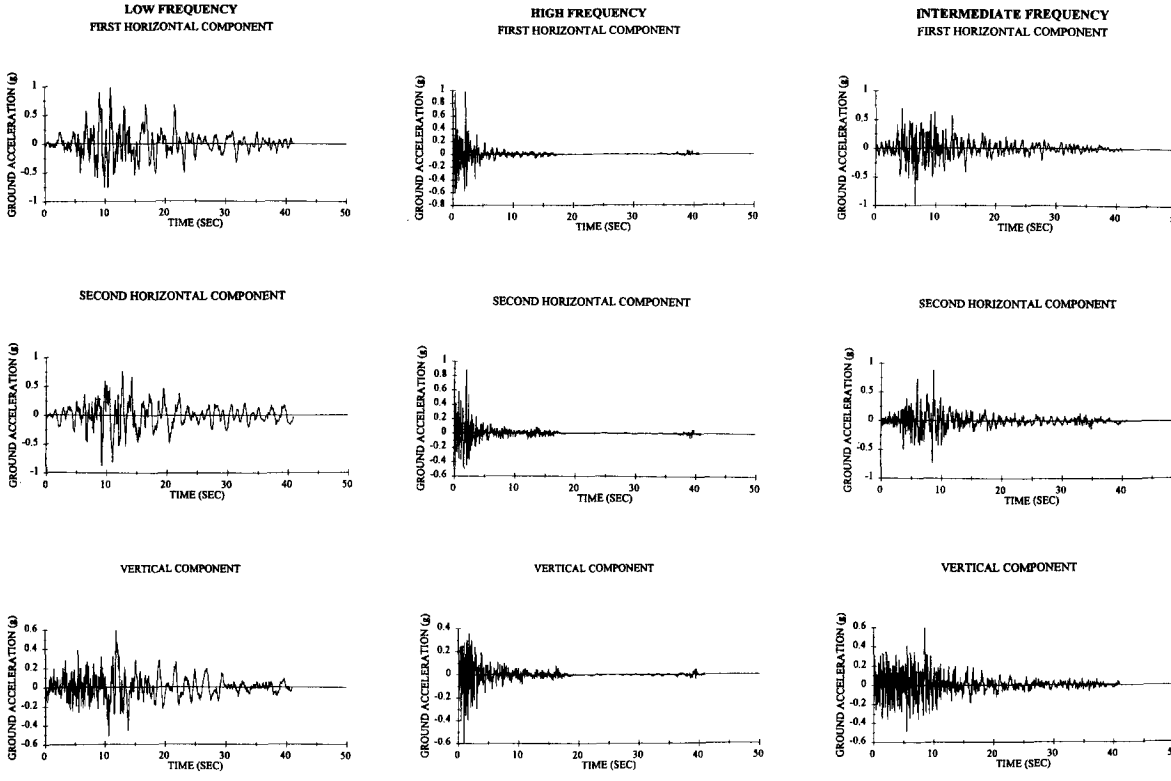

Fig. 8 Synthetic ground acceleration records.

Deck and tower seismic induced internal forces are calculated for the two models. These quantities are normalized with respect to the maximum corresponding dead load internal forces. For example, the normalized GFRP bridge deck seismic moment is calculated by dividing the GFRP bridge deck seismic moment at each section by the maximum GFRP bridge deck dead load moment. To have a base for the comparisons, the live load internal forces for both models are also calculated and normalized with respect to the dead load internal forces. The normalized live load internal forces were included because they are usually replaced by the seismic forces in the design load combinations. Figs. 9 and 10 show the normalized seismic and live load

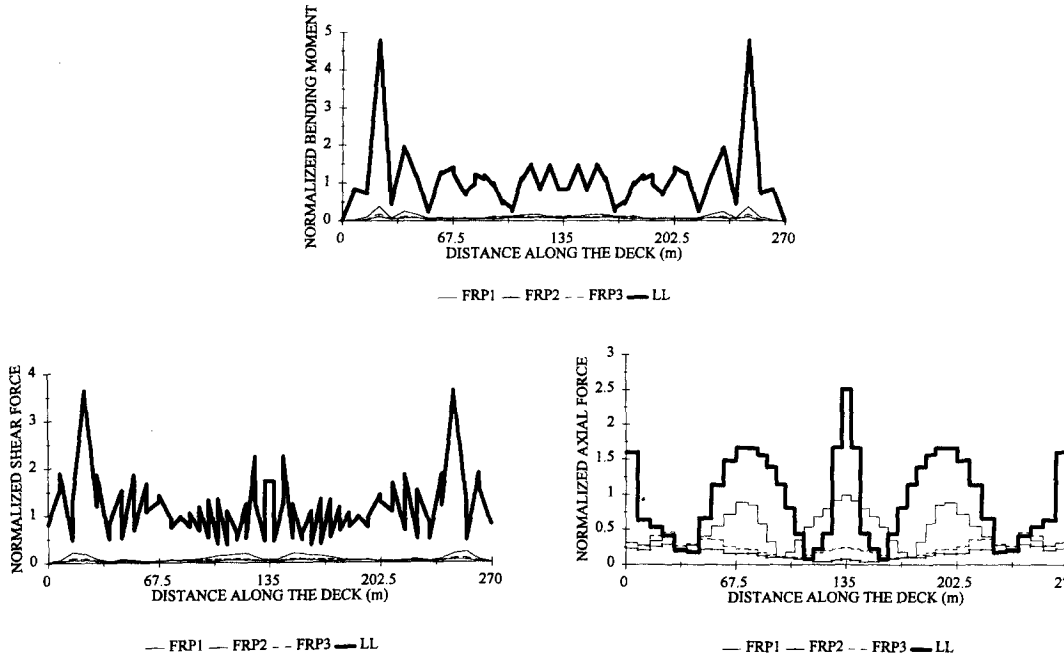

Fig. 9 Normalized internal forces for the GFRP deck.

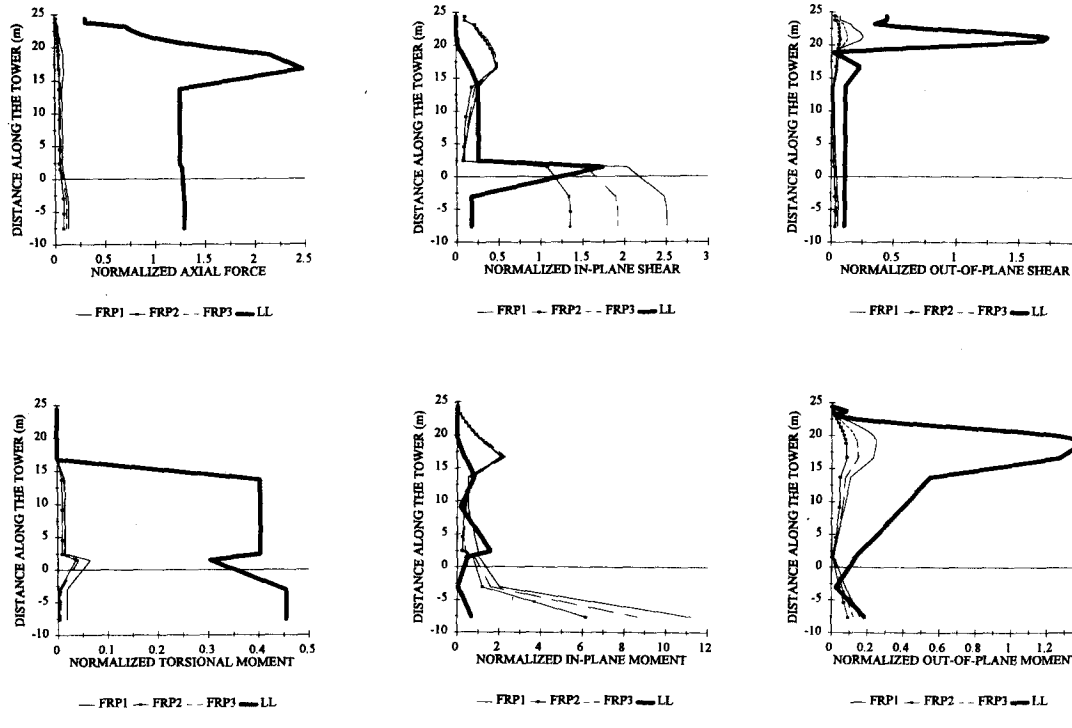

Fig. 10 Normalized internal forces of the GFRP tower.

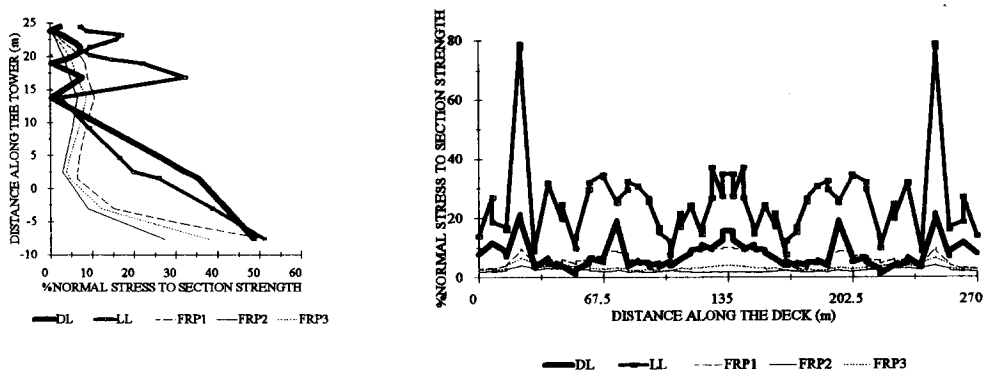

Fig. 11 Normalized normal stress of the GFRP bridge.

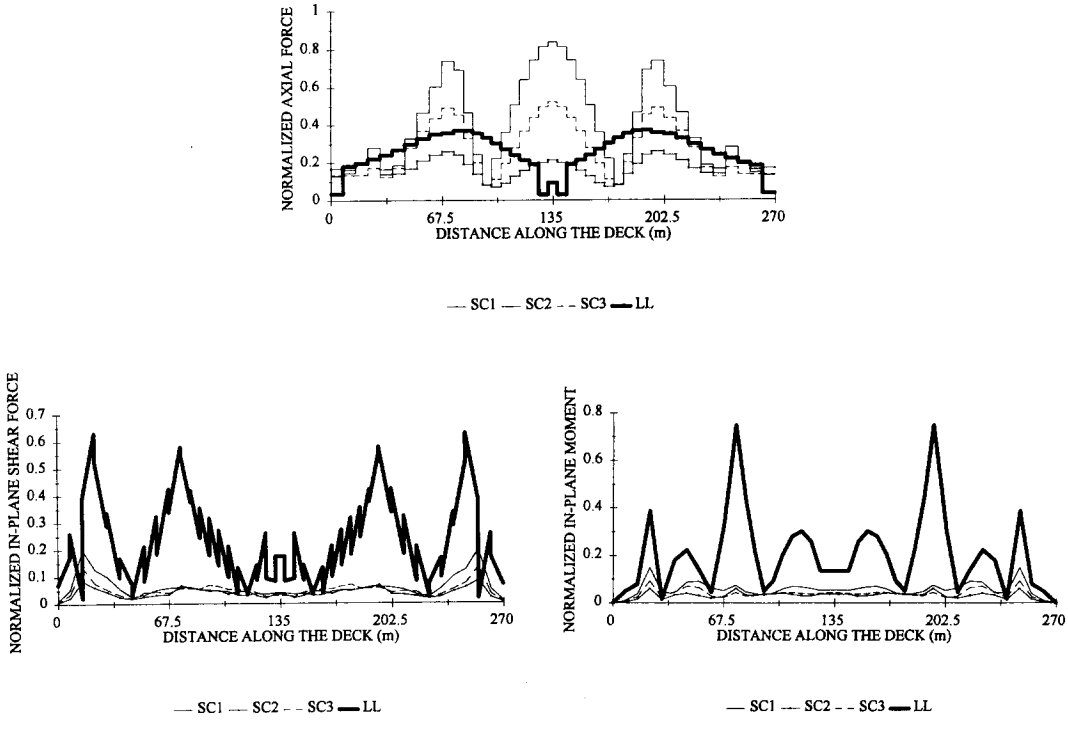

Fig. 12 Normalized internal forces of the SC deck.

internal forces for the GFRP model. To compare the induced internal stresses an alternative procedure was used, in which, the normal stresses at the different bridge sections were calculated and then divided by the design normal strength of the corresponding sections. Fig. 11 shows the normalized normal stress for the GFRP alternative. Figs. 12, 13 show the normalized seismic and live load internal forces for the SC model. Fig. 14 shows the normalized normal stress for the SC alternative. The response curves on Figs. 9-14 with designation ending with the number "1" refer to the seismic response calculated for the low A/V 0.1 g reference input, with designation

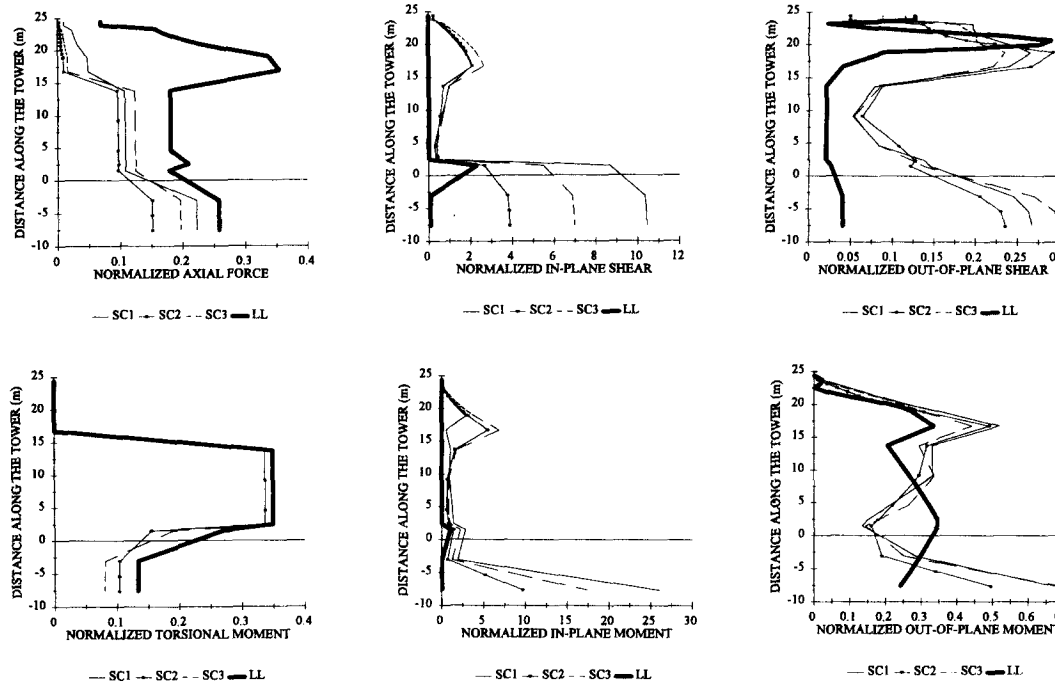

Fig. 13 Normalized internal forces of the SC tower.

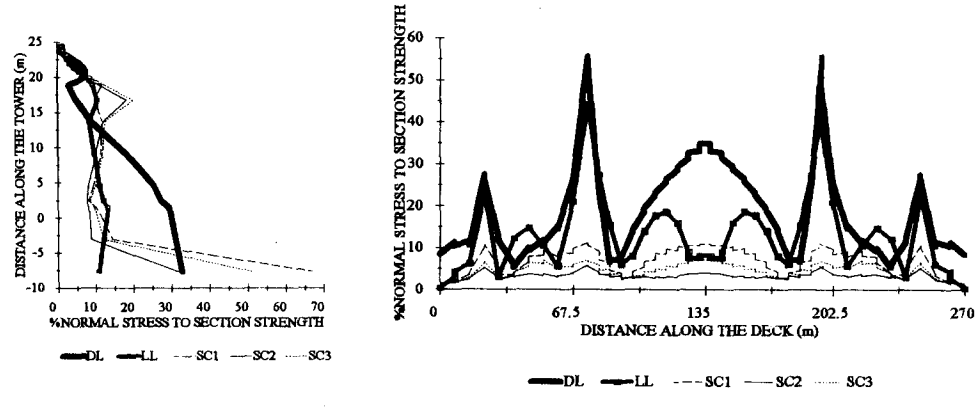

Fig. 14 Normalized normal stress of the SC bridge.

ending with the number "2" refer to the seismic response calculated for the high *A/V* 0.1 g reference input, and with designation ending with the number "3" refer to the seismic response calculated for the intermediate *A/V* 0.1 g reference input.

6. Discussion

The in-plane towers' base shear is calculated for the two design alternatives. The percentage

of tower base shear with respect to the total weight of the respective design alternative is calculated. It was found that the GFRP alternative has in-plane tower base shear that ranges between one percent (high A/V) and two percent (low A/V) of the total weight. The ratio ranges between one percent (high A/V) and four percent (low A/V) for the SC alternative. The close values of the base shear percentage between the two alternatives is surprising however, the combination of the light weight and relatively low stiffness of the GFRP alternative explains these close values. A more detailed analysis was adopted after this basic assessment by looking into the internal forces developed in both alternatives by the seismic excitation. To obtain meaningful comparisons it was decided to calculate the aforementioned normalized internal forces and stresses.

The deck normalized seismic moment and shear force are negligible compared to normalized live load moment and shear force for both design alternatives. However, the GFRP deck has higher normalized seismic moment and shear force than SC alternative as shown in Figs. 9 and 12. The normalized seismic deck normal force for the GFRP alternative is close in value to that of the SC alternative. As expected, the normalized live load deck internal forces for the GFRP alternative are much higher than those of the SC alternative. This may be attributed to the light weight of the GFRP alternative which gives a higher live load/dead load ratio than the SC alternative.

The towers' responses to the 0.1 g reference input are significant. The tower bases of both design alternatives are subjected to very high out-of-plane shear forces and in-plane bending moments. Normalized bending moments of up to 11 are reported for the GFRP alternative and up to 25 are reported for the SC alternative. These values are very high compared to the normalized live load moments which have values less than one as shown in Figs. 10 and 13. The normalized shear forces reach the value of 2.5 for the GFRP alternative and 10 for the SC alternative. These normalized seismic shear force values are much higher than those of the normalized live load shear forces that have values less than one as shown in Figs. 10 and 13. This means that special seismic design provisions are required even for this relatively low level of ground excitation (the 0.1 g reference input) for both design alternatives in the form of either special energy dissipation devices or special tower base design.

On examining Figs. 11, 14 it can be concluded that normalized seismic stresses are negligible in the bridge decks of the two alternatives compared to dead load and live load normalized stresses. The normalized dead load stress comprises only 20% of the section strength and live load stress comprises 80% of the section strength for the GFRP alternative. This is attributed to the light weight nature of the material. On the other hand, the normalized dead load stress comprises more than 50% of the section strength for the SC alternative. The normalized seismic internal stress at the tower's base of the GFRP alternative for the low frequency content ground motion is slightly higher than the live load normalized internal stress. This means that the design and detailing of the tower base for GFRP bridges at low A/V locations (with peak ground acceleration of only 0.1 g) will be governed by the seismic internal stresses. The normalized seismic internal stress at the tower's base for the SC alternative induced by all three ground motions are higher than live load normal stresses.

The frequency content of the ground acceleration affected the towers' responses. The low frequency input causes the highest tower internal forces while the high frequency input causes the lowest internal forces. The towers normalized seismic moments and shear forces due to the low A/V 0.1 g reference input have exceeded double the values of the towers normalized seismic

moments and shear forces due to the high *A/V* 0.1 g reference input. This may be explained by examining the spectral shapes of the three *A/V* categories used in this study. The frequency range of the two design alternatives matches the tails of the spectra of Fig. 7 which are characterized by high spectral ordinates for the low frequency input then lower for the intermediate and the lowest for the high frequency input.

This work was carried out using ground acceleration records that have maximum ground acceleration of 0.1 g as a reference and to explore the characteristics of the seismic response of the GFRP alternative. Higher ground motion accelerations are expected in a few regions of the United States for which it is expected that the seismic response of the GFRP alternative will be much higher and appropriate seismic design provisions should be applied.

7. Conclusions

This investigation has been conducted to study the unique dynamic characteristics of a GFRP cable-stayed bridge and their effects on the seismic response of such complex 3-D structure. The study showed that GFRP cable-stayed bridges are generally more flexible than conventional Steel-Concrete (SC) cable-stayed bridges. Many modes of the GFRP have no match with the SC modes. The extracted mode shapes showed that the GFRP is considerably more flexible than the SC alternative in the transverse and longitudinal directions. Although the GFRP alternative has higher fundamental vertical frequency than the SC alternative its deck vertical response is merely a one mode response quantity because of the high amount of the effective modal mass for that mode shape. The same conclusion applies to the longitudinal seismic response of the GFRP towers.

The seismic response of the GFRP bridge quantified by the ratio of every internal force divided by the corresponding maximum value of the dead load internal force has proven to be significant even for ground excitations with peak ground acceleration as low as 0.1 g. At the tower bases the seismic internal forces are higher than live load induced internal forces which would make the design process governed by the seismic forces. The base shear at the tower base is estimated to range between one and two percent of the dead weight of the total structure depending on the frequency content of the ground acceleration. The SC base shear ranges between one and four percent of the total weight of the structure. This is caused by the new deformation shapes of the GFRP and the frequencies of its mode shapes. It is thus concluded that GFRP cable stayed bridges to be constructed at locations with seismic activity should be given enough care in the analysis, design, and detailing to sustain the expected seismic loads.

Acknowledgements

This study is supported in part by the University of Nebraska-Lincoln through its Center for Infrastructure Research and the City of Lincoln. The financial support of these two agencies is gratefully acknowledged.

References

_____ (1984), *Plastic Design Manual,* ASCE.

Abdel-Ghaffar, A.M. and Nazmy, A.S., (1987), "Effects of three dimensionality and non-linearity on

the dynamic and seismic behaviour of cable-stayed bridges", *Bridges and Transmission Line Structures,* ed. *Lambert Tall,* 389-404.

Abdel-Ghaffar, A.M. and Khalifa, M.A., (1991), "Importance of cable-vibration in dynamics of cable-stayed bridges", *Proc. ASCE, Journal of Structural Engineering,* **117**(11), 2571-2589.

Habibullah, A. and Wilson, (1989), *SAP90: A Series of Computer Programs for the Finite Element Analysis of Structures,* Computers and Structures Inc., Berkely, California.

Head, P.R. (1992), "Design method and bridge forms for the cost effective use of advanced composites in bridges", *Advanced Composite Materials in Bridges and Structures, ASCE*, Neale, K.W. and Labossiere, P. ed., 15-30.

Heger, F.J. and Chambers, R.E. (1984), "Design with structural plastics", *Building Structural Design Handbook,* John Wiley and Sons, New York.

Hodhod, O.A. (1993), "Dynamic and seismic characteristics of cable-stayed bridges", PhD Thesis, McMaster University, Hamilton, Ontario.

Khalifa, M.A. and Tadros, M.K. (1994), "The world's longest cable-stayed foot-bridge using fiber reinforced plastics", *Proceedings of the Third Materials Engineering Conference. ASCE,* Basham, K.D. ed., San Diego, California, 207-214.

Khalifa, M.A., Kuska, S.S.B. and Krieger, J. (1993), "Bridges constructed using fiber reinforced plastics", *Concrete International,* **15**(6), 43-47.

Mossallam, A.S. and Chambers, R.E. (1994), "Design procedure for predicting creep and recovery of pultruded composites", *50th Annual Conference,* Composites Institute, The Society of the Plastics Industry.

Mossallam, A.S. (1993), "Pultruded composites: materials for the 21st century", *Plastics for the 21st Century Construction, ASCE*, Chambers, R.E. ed., 23-55.

Mossallam, A.S. and Abdelhamid, M.K. (1993), "Dynamic behavior of PFRP structural sections", *Composite Material Technology, ASME*, PD-53, 37-43.

Naumoski, N., Tso, W.K. and Heidebrecht, A.C. (1989), "A selection of representative strong motion earthquake records having different A/V ratios", Earthquake Engineering Research Group, *EERG Report* 88-01, McMaster University, Hamilton, Ontario.

Nazmy, A.S. and Abdel-Ghaffar, A.M. (1987), "Seismic response analysis of cable-stayed bridges subjected to uniform and multiple-support excitation", Report No. 87-SM-1, Princeton University.

Nazmy, A.S. and Abdel-Ghaffar, A.M. (1990a), "Non-linear earthquake response analysis of long span cable-stayed bridges: theory", *International Journal of Earthquake Engineering and Structural Dynamics,* **19**, 45-62.

Nazmy, A.S. and Abdel-Ghaffar, A.M. (1990b), "Non-linear earthquake response analysis of long span cable-stayed bridges: application", *International Journal of Earthquake Engineering and Structural Dynamics,* **19**, 63-76.

Scanlan, R.H. (1987), "Aspects of wind and earthquake dynamics of cable-stayed bridges", *Bridges and Transmission Line Structures, ASCE*, L. Tall, ed., 329-340.

Seible, F., Hegemier, G.A. and Nagy, G. (1994), "The aberfeldy glass fiber composite pedestrian bridge", *Advanced Composite Technology Transfer Consortium,* Report No. ACTT-94/01, University of California, San Diego.

Seible, F. (1994) Personal Communication.

Seible, F., Sun, Z. and Ma, G. (1993), "Galss fiber reinforced composite bridges in china" *Advanced Composite Technology Transfer Consortium,* Report No. ACTT-93/01, University of California, San Diego.

Tso, W.K., Zhu, T.J. and Heidebrecht, A.C. (1992), "Engineering implication of ground motion A/V ratio", *Soil Dynamics and Earthquake Engineering,* **11**, 133-144.

Wilson, J.C. and Gravelle, W. (1991), "Modeling of a cable-stayed bridge for dynamic analysis", *International Journal of Earthquake Engineering and Structural Dynamics,* **20**, 707-721.

Wilson, J.C. and Liu, T. (1991), "Ambient vibration measurements on a cable-stayed bridge", *International Journal of Earthquake Engineering and Structural Dynamics,* **20**, 723-747.